Letter | Editors' Suggestion

Dynamics of a fractal set of first-order magnetic phase transitions in frustrated Lu_2CoMnO_6

Adra Carr,[1,2,*] John Bowlan,[3,*] Claudio Mazzoli,[4,*] Colby Walker,[2,5] Xiaxin Ding,[1,†] Andi Barbour,[4] Wen Hu,[4] Stuart Wilkins,[4] Jong Hyuk Kim,[6] Nara Lee,[6] Young Jai Choi,[6] Shi-Zeng Lin,[7] Richard L. Sandberg,[2,5] and Vivien S. Zapf[1]

[1]*National High Magnetic Field Laboratory, Los Alamos National Laboratory (LANL), Los Alamos, New Mexico 87545, USA*

[2]*Center for Integrated Nanotechnologies, LANL, Los Alamos, New Mexico 87545, USA*

[3]*C-PCS, LANL, Los Alamos, New Mexico 87545, USA*

[4]*NSLS-II, Brookhaven National Laboratory, Upton, New York 11973, USA*

[5]*Department of Physics and Astronomy, Brigham Young University, Provo, Utah 84602, USA*

[6]*Department of Physics, Yonsei University, Seoul 03722, Korea*

[7]*Theoretical Division, LANL, Los Alamos, New Mexico 87545, USA*

(Received 28 May 2020; revised 10 December 2020; accepted 13 January 2021; published 4 February 2021)

The axial next-nearest-neighbor Ising model predicts a fractal (infinite) set of phases with incommensurate wave vectors that are separated by first-order phase boundaries. This complexity results from a simple frustration condition between nearest- and next-nearest-neighbor interactions along a chain of Ising spins. Using x-ray photon correlation spectroscopy (XPCS), we investigate the surprising antiferromagnetic dynamics that emerge from such a complex phase diagram over a wide range of temperatures. We present XPCS measurements of the frustrated magnetic chain compound Lu_2CoMnO_6 and Monte Carlo simulations. Incommensurate magnetic Bragg peaks slide towards commensurate "up-up-down-down" spin order with decreasing temperature and increasing time. Both simulation and experiment support a counterintuitive "upside-down" temperature dependence of the magnetic dynamics: at higher temperatures in the region of first-order phase boundaries, slower dynamics are observed where the speckle maintains its coherence. At the lowest temperatures, where part of the sample adopts commensurate order, the dynamics speed up and result in fast decoherence.

DOI: 10.1103/PhysRevB.103.L060401

In frustrated magnets, seemingly simple competition between spin interactions can create profound complexity. The axial next-nearest-neighbor Ising (ANNNI) model [1–3] is a classic model of frustration in which nearest-neighbor ferromagnetic (FM) interactions and next-nearest-neighbor antiferromagnetic (AFM) interactions compete with each other along chains of Ising spins. As an ANNNI system is cooled below T_N, it passes through a fractal set of first-order phase boundaries that separate AFM phases with different incommensurate (ICM) wave vectors, referred to as the "devil's staircase" or "devil's flower" [1,2]. At a lower temperature, a commensurate (CM) wave vector emerges such as "up-up-down-down" spin ordering along the chains of Ising spins.

The existence of such a large number of first-order phase transitions should produce interesting dynamics of the magnetic system. However, historically, the dynamics of antiferromagnets, frustrated or otherwise, has been difficult to study due to their domains having no net magnetization. Thus, the development of x-ray-based techniques at light sources presents unique opportunities to probe AFM domain dynamics [4–11]. In particular, x-ray photon correlation spectroscopy (XPCS) of Bragg scattering that is resonantly tuned to magnetic ions can detect AFM order and its inhomogeneities in time (seconds to hours) and space (nanometers to microns) [12–15]. This is important since frustrated systems evolve between different, nearly degenerate states, creating slow dynamics and inhomogeneities. XPCS has led to, e.g., observations of the dynamics of spin density waves in Cr [12] and of spin-helix phases in Dy [13,14]. Thus far, XPCS studies of antiferromagnets have found that when samples are cooled slightly below the Néel temperature $T < T_N$, the AFM dynamics become slow or freeze, as would be intuitively expected from thermal activation [12–14].

In this work, however, we use XPCS to observe very slow dynamics over a broad range of temperature down to a quarter of T_N in highly frustrated Lu_2CoMnO_6 [16–19]. Moreover, we provide a theoretical framework to understand the dynamics using Monte Carlo simulations of the ANNNI model. This compound is known to be a likely ANNNI system based on previous measurements of thermodynamic properties, muon spin resonance (μsR), and neutron diffraction [20,21]. Co^{2+} and Mn^{4+} with $S = 3/2$ spins occupy oxygen cages, and the two magnetic ions alternate along the a, b, and c axes [16] with lattice spacing of $a = 5.1638(1)$ Å, $b = 5.5467(1)$ Å, $c = 7.4153(1)$ Å. A powder neutron diffraction study found that the magnetic state at 4 K consists of Co ↑ Mn ↑ Co ↓ Mn ↓ with both the spins and wave vector along the c axis and a slight incommensurability with $\vec{k} \approx [0.0223(8), 0.0098(7), 0.5]$ [see Fig. 1(a)] [16]. Since the compound is a type II multiferroic [16–19], previous studies used both the magnetization and electric polarization to determine that this system has slow dynamics, down to hour

*These authors contributed equally to this work.

†Present address: Idaho National Laboratory, Idaho Falls, Idaho 83415, USA.

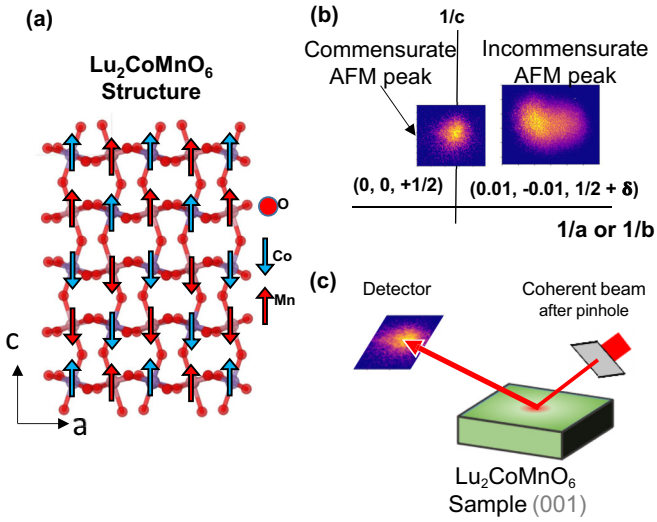

FIG. 1. (a) Structure of Lu_2CoMnO_6 with spins (arrows) and Lu atoms omitted. (b) Incommensurate and commensurate Bragg peaks, shown with their respective reciprocal space wave vector. (c) Experimental setup of a resonant XPCS experiment, with the c axis normal to the illuminated sample face.

timescales, as well as frequency dependence of the above quantities. These dynamics were observed below $T_N = 48$ K and above $T_{\rm Hyst} = 30$–35 K, where hysteresis emerges in the magnetization and electric polarization on hour timescales. Dynamics between picosecond and microsecond timescales were also uncovered by measuring μSR and neutron diffraction [21]. Below $T_{\rm Hyst}$, hysteresis appears in the magnetization and electric polarization, suggesting that AFM and field-induced FM domains become pinned below this temperature by spin-lattice interactions [16,19].

XPCS data were collected on a millimeter-sized single crystal of Lu_2CoMnO_6 [18] at the Coherent Soft X-ray Scattering (CSX, 23-ID-1) beamline at the National Synchrotron Light Source-II (NSLS-II) [15] during three different beam times. This beamline has previously demonstrated sufficient stability for XPCS studies over multiple hours [15]. All data presented here are for one beam time and one sample, while data for two additional beam times and one additional sample are presented in the Supplemental Material [22] (see also Refs. [23–25] therein). The crystal was polished on the (001) faces down to 0.3-μm grit and mounted with the (001) face upward on a copper sample holder with silver paint. Coherent x rays passed through a 10-μm pinhole, then resonantly Bragg scattered off the Co or Mn ions in the geometry shown in Fig. 1. Speckle in the Bragg peak was detected using a two-dimensional (2D) detector and serves as a measure of AFM inhomogeneities. The autocorrelation function of this speckle can be analyzed to extract statistical information. Each speckle pattern was recorded at a fixed T every 3.25 s for up to 3 h, after verifying thermalization (see the Supplemental Material (SM) [22]). The dynamics of the speckle pattern and thus the domain patterns which they encode are analyzed by computing the autocorrelation function $g^{(2)}(\vec{q},\tau)$ of the speckle intensity $I(\vec{q},t)$: $g^{(2)}(\vec{q},\tau) = \langle I(\vec{q},t)I(\vec{q},t+\tau)\rangle / \langle I(\vec{q},t)\rangle^2$. Here, the intensities $I(\vec{q},t)$ and $I(\vec{q},t+\tau)$ are extracted for a particular momentum vector $\vec{q}$ at times t and $t+\tau$, with τ being a delay time and angle brackets denoting time averaging.

We investigate the two satellite ICM Bragg peaks $\vec{k} = [\pm\delta, \mp\delta, 1/2 \mp \epsilon]$ and a CM Bragg peak $\vec{k} = [0, 0, 1/2]$, where the CM peak corresponds to the up-up-down-down ordering. δ and ϵ are in the range of 0.01 or lower and decrease with T [22]. Data were taken at Co and Mn edges for σ and π x-ray polarization, and a complete XPCS data set was taken at the Co edge with π polarization since it had the largest magnitude.

We find that above $T_{\rm Hyst}$ (the region where physical properties have no hysteresis in T or magnetic field) the nominal CM [0, 0, 1/2] Bragg peak has no resolvable energy dependence near the Co or Mn L_3 edges, showing that this peak is not at a magnetic resonance. We conclude that it is dominated by the second harmonic of the x-ray beam diffracting off the [0,0,1] lattice peak. However, below $T_{\rm Hyst}$ this Bragg peak acquires a strong resonance at the Co and Mn L_3 edges. Thus, this Bragg peak becomes dominated by the [0, 0, 1/2] magnetic peak. The predominance of the spin rather than the charge scattering channel at the lowest temperature is also confirmed by comparing σ and π polarizations (see the SM [22]). Meanwhile, the ICM peak can be observed only at the Co and Mn L_3 edges at all $T < T_N$, both above and below $T_{\rm Hyst}$, proving its magnetic character. The fact that the CM peak abruptly acquires a magnetic component below $T_{\rm Hyst}$ may indicate that part of the sample evolves all the way to the CM order as T is lowered, while another part of the sample remains trapped in a state described by an ICM wave vector. Evidence for this is also found in intermittent pinning of parts of the ICM peak as the temperature is lowered (see Fig. 1 and the movie in the SM). The wave vectors of the CM and ICM peaks were reproducible at different locations on the sample, although the ICM peaks were not always visible.

We find that for the ICM peak, there is a small T dependence of δ and ϵ (see the SM [22]) such that the ICM peaks approaches the CM $\vec{k} = [0, 0, 1/2]$ position as T is lowered from T_N to $T_{\rm Hyst}$, as predicted for the ANNNI model. We also noted a significant drift in the magnetic ICM Bragg peak position over time for $T > T_{\rm Hyst}$. This drift is shown in Fig. 2 over a roughly 2-h period, with a lack of drift in CM peak shown for comparison. A similar drift of the ICM peak towards the CM peak was observed in the potential ANNNI spin chain compound $Ca_3Co_2O_6$ [20,26,27], where it was attributed to the inability of the system to reach its stable ICM wave vector after a decrease in T due to very slow dynamics.

Figures 3(a) and 3(b) show the dynamics of speckle in the ICM peak at the Co edge at 778 eV at $T = 35$ K and 24 K, just above and below $T_{\rm Hyst} = 30$ K. On the right are waterfall plots, showing an average over a vertical stripe through the center of the Bragg peak 1.4×10^{-4} Å^{-1} wide (2 pixels) vs time. The ICM speckle pattern is relatively unchanged at 35 K over the 3 h, whereas at 25 K the speckle shifts and decorrelates on this timescale.

In Figs. 3(c) and 3(d) the normalized intermediate scattering function $g^{(2)} - 1$ (the autocorrelation function between the signal at different times) is shown at $T = 25$, 35, and 55 K. The CM peak resonates at the Co and Mn edges for 25 K, while the ICM peak resonates at 25 and 35 K. The

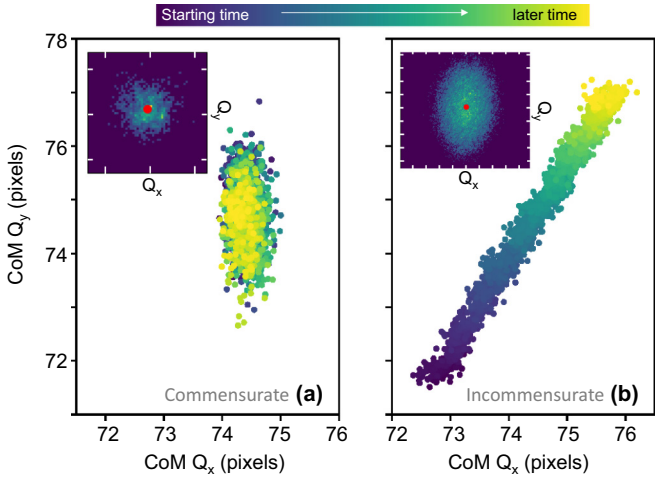

FIG. 2. Center of mass (CoM) of (a) CM and (b) ICM peaks at 35 K shown in detector pixels (1 pixel $= 7 \times 10^{-5}$ Å^{-1}). The color denotes the relative position in time over 1.8 h. Insets show the Bragg peak, with the red dot indicating the center of mass. White hash marks denote 20-pixel intervals.

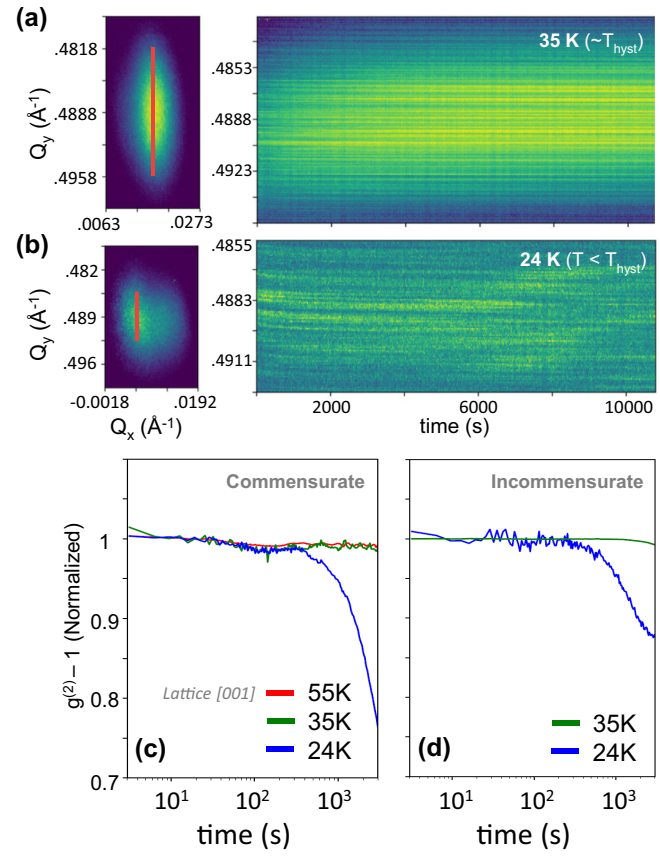

FIG. 3. (a) Waterfall plot (right) showing the cross section of a π ICM Bragg peak at 35 K vs time, where the cross section is integrated over the red line out defined on the left. (b) Similar waterfall plot for 24 K. Normalized autocorrelation function ($g^{(2)} - 1$) vs time for (c) the CM peak at [0, 0, 1/2] and (d) ICM peak at [0.0087, −0.0042, 0.489] and [0.0168, −0.006, 0.4888] at 35 K. All data are shown for the Co L_3 edge with π polarization. The data at 55 K are above T_N and thus represent the [001] structural peak in the first harmonic of the x-ray beam.

temperature 55 K is above T_N, and therefore, no magnetic signal is present in the data, while the reported signal in the CM position at this T is attributed to the lattice, as already discussed. The autocorrelation is normalized to the average of $g^{(2)} - 1$ within the first 30 s of integration, serving as a representative baseline. The non-normalized autocorrelation also showed a clear decrease in speckle contrast with decreasing T, consistent with the emergence of fast (microsecond) relaxation timescales observed in other work [21]. Non-normalized autocorrelations as well as the exact regions of interest (ROIs) used can be found in the SM [22]. Autocorrelation functions for other subregions of the CM Bragg peak were unable to discern notably separate dynamics between the central and outer portions of the Bragg peak (see the SM [22]).

Therefore, by means of XPCS we determine that the speckle from domains in the magnetic ICM and CM peaks at 25 K (below T_{Hyst}) decorrelate significantly more rapidly than at 35 K. This result is reproduced in an additional data set shown in the SM [22]. While this observation is counterintuitive since dynamics usually freeze at low T, it is, in fact, a prediction of the ANNNI model due to the presence of a devil's staircase of first-order phase transitions at intermediate temperatures [1–3]. These dense first-order phase boundaries can lead to an effective pinning of ICM wave vectors and consequently slower magnetic dynamics. Below T_{Hyst}, on the other hand, large stable magnetic domains form, and the dynamic speckle behavior is produced by faster local fluctuations within each domain.

In the following, we calculate the dynamics in an ANNNI Monte Carlo model. Monte Carlo simulations of the dynamic behavior of the ANNNI model were performed to compare with the experimental data. We note that in Lu_2CoMnO_6 there are two magnetic ions instead of one, which is a deviation from the classic single-ion ANNNI model. We perform simulations for the two-ion ANNNI model (here) and compare the results to the single-ion model (see the SM [22]) to confirm that the dynamics are similar. Moreover, we perform calculations for 2D and three-dimensional (3D) models (see the SM [22]) and find similar dynamics.

The in-plane ordering wave vector is small; thus, we assume a simple nearest-neighbor FM interaction in the *a*-*b* plane. The spin Hamiltonian is expressed as

$$\mathcal{H} = -J_1 \sum_{NN} \sigma_i S_j^z - J_2 \sum_{NNN} \sigma_i \sigma_j - J_2' \sum_{NNN} \mathbf{S}_i \cdot \mathbf{S}_j - A \sum_i \left(S_i^z\right)^2,$$

where $\sigma_j = \pm 1$ is the Co^{2+} Ising spin and $|\mathbf{S_j}| = 1$ is the Mn^{4+} Heisenberg spin with an easy-axis anisotropy, $A > 0$. $\mathbf{S_j}$ and σ_j form two sublattices of the square lattice, as shown in Fig. 4(a). $J_1 > 0$ is the nearest-neighbor FM interaction, and $J_2 < 0$ and $J_2' < 0$ are the next-nearest-neighbor AFM interaction along the c axis. We choose $J_2 = J_2' = -0.6J_1$ and $A = J_1$. We employ a 2D model corresponding to the *a*-*c* plane of Lu_2CoMnO_6 and perform Monte Carlo simulations of $\mathcal{H}$ with the standard Metropolis algorithm.

The calculated ordering wave vector Q vs T is shown in Fig. 4(a). Because of the finite-size effect, Q changes stepwise with T. There are peaks in the calculated specific heat when Q changes which correspond to the first-order phase

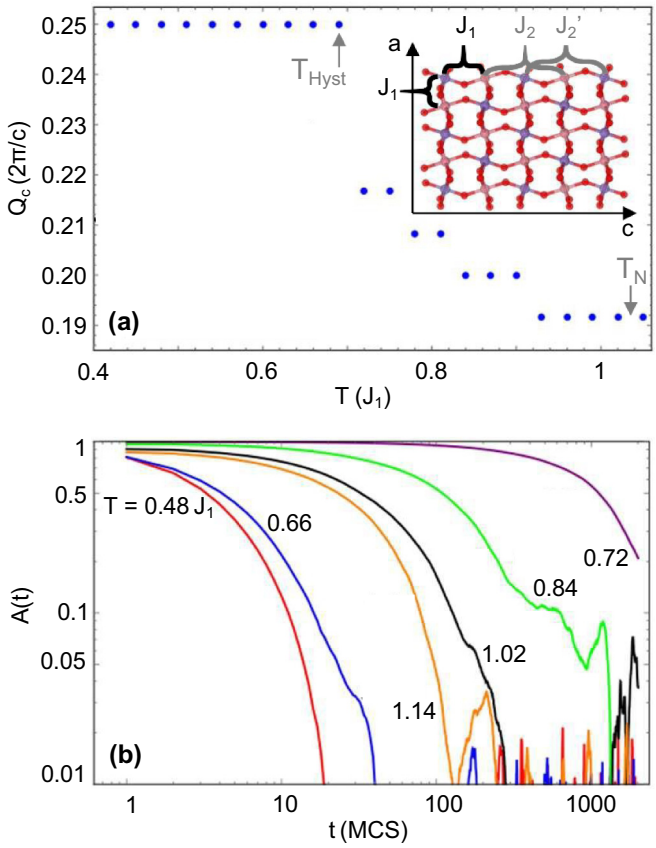

FIG. 4. (a) Monte Carlo simulations of the ICM AFM wave vector Q vs T, obtained by slowly cooling to $T = 0$ and then heating. The inset shows the magnetic model with nearest- and next-nearest-neighbor magnetic interactions. (b) Calculated spin autocorrelation function $A(t)$ at fixed $Q = 0.25 \times 2\pi/c$ vs time for varying T. Time t is shown in units of Monte Carlo sweep (MCS).

transition between different Q states. The first-order phase transition implies slow dynamics in the ICM phase. For increasing system size, Q changes quasicontinuously through many weak first-order transitions. To capture the dynamics, we compute the autocorrelation function of the spin structure factor $S(Q,t) \equiv \langle M_z(Q,t)M_z(-Q,t)\rangle$, represented as

$$A(t) = \int_0^\tau dt_1[\mathcal{S}(t_1)-\bar{\mathcal{S}}][\mathcal{S}(t+t_1)-\bar{\mathcal{S}}] \Big/ \int_0^\tau dt_1[\mathcal{S}(t_1)-\bar{\mathcal{S}}]^2,$$

where M_z is the z component of the magnetization at wave vector Q and $\langle\cdots\rangle$ denotes thermal averaging. Here t is the Monte Carlo time, τ is the total simulation time, and $\bar{\mathcal{S}}$ is the mean value of $S(Q,t)$. The results, displayed in Fig. 4(b), show that the dynamics for $T_N < T < T_{\rm Hyst}$ are extremely slow, slower than the region below $T_{\rm Hyst}$. The correlation time is particularly long at the first-order phase transition point.

The simulations of the dynamics are qualitatively consistent with the XPCS results. The theory and experiment both show "inverted" dynamics, where the speckle decorrelates faster below $T_{\rm Hyst}$ than above it.

In conclusion, we observed dynamics of speckle in CM and ICM peaks over a very broad range of temperature down to a quarter of T_N. Surprisingly, these dynamics are inverted in temperature from ordinary magnets, with fast decorrelation at low T and slow decorrelation at high T. Monte Carlo simulations showed that these unusual dynamics are predicted by the ANNNI model for both one and two types of magnetic ions. Above $T_{\rm Hyst}$ the ANNNI model predicts many (theoretically infinite) first-order phase transitions occurring at closely spaced temperatures whose domain boundaries pin the ICM wave vectors, creating slow dynamics. This manifests as a lack of decorrelation in the speckle measured. Though the ICM wave vectors do not decorrelate, they drift in the direction of the CM wave vector for at least 3 h after a change in T, as has been seen in other similar ANNNI systems [27]. Below $T_{\rm Hyst}$, the system has stable pinned domains, and so the dynamics are dominated by fast fluctuations within each domain and rapid decorrelation of the speckle. Previous XPCS investigations of Dy and Cr also showed ICM order due to frustration between nearest and next-nearest neighbors [12,14]. However, these systems do not have Ising spins and are thus not examples of the ANNNI model. In these compounds, dynamics were observed only in the immediate vicinity of T_N.

Our work demonstrates that magnetic frustration can produce unexpected dynamics over a wide range of temperatures detectable by XPCS. Though the ANNNI model of frustration was first developed in the 1980s, we can now investigate its ramifications for the dynamics of antiferromagnetic inhomogeneities using both simulation and experiments.

We are grateful to A. Tripathi, B. Pound, and S. Chikara for helpful experimental aid and to C. Batista and W. Selke for valuable discussions. Scientific work began in the LDRD program at LANL and was completed (in particular, the theoretical work) as part of the US DOE, Office of Science, Basic Energy Sciences, Materials Sciences and Engineering Division, Condensed Matter Theory Program. This research utilized beamline 23-ID-1 of NSLS II, a US DOE Office of Science User Facility operated for the DOE Office of Science by Brookhaven National Laboratory under Contract No. DE-SC0012704, as well as the facilities of CINT, an Office of Science User Facility operated for the US DOE Office of Science by LANL, and, finally, the facilities of the NHMFL, funded by the US NSF through Cooperative Grant No. DMR-1157490, the U.S. DOE, and the state of Florida. Sample growth efforts at Yonsei University were supported by the National Research Foundation of Korea, Grant No. NRF-2017R1A5A1014862 (SRC program: vdWMRC center, Grants No. NRF-2018R1C1B6006859 and No. NRF-2019R1A2C2002601).

[1] P. Bak and M. H. Jensen, J. Phys. C **13**, L881 (1980).
[2] P. Bak, Rep. Prog. Phys. **45**, 587 (1982).
[3] W. Selke, Phys. Rep. **170**, 213 (1988).

[4] M. M. Schwickert, G. Y. Guo, M. A. Tomaz, W. L. O'Brien, and G. R. Harp, Phys. Rev. B **58**, R4289 (1998).

[5] J. Kortright, D. Awschalom, J. Stöhr, S. Bader, Y. Idzerda, S. Parkin, I. K. Schuller, and H.-C. Siegmann, J. Magn. Magn. Mater. **207**, 7 (1999).

[6] F. Nolting, A. Scholl, and J. Stöhr, Nature (London) **405**, 767 (2000).

[7] J. Stöhr and H. C. Siegmann, *Magnetism: From Fundamentals to Nanoscale Dynamics* (Springer, Berlin, 2006), Vol. 1.

[8] T. Zhao, A. Scholl, F. Zavaliche, K. Lee, M. Barry, A. Doran, M. P. Cruz, Y. H. Chu, C. Ederer, N. A. Spaldin, R. R. Das, D. M. Kim, S. H. Baek, C. B. Eom, and R. Ramesh, Nat. Mater. **5**, 823 (2006).

[9] M. G. Kim, H. Miao, B. Gao, S.-W. Cheong, C. Mazzoli, A. Barbour, W. Hu, S. B. Wilkins, I. K. Robinson, M. P. M. Dean, and V. Kiryukhin, Nat. Commun. **9**, 5013 (2018).

[10] T. Kołodziej, I. Biało, W. Tabiś, M. Zubko, J. Żukrowski, K. Łątka, J. E. Lorenzo, C. Mazzoli, Z. Kąkol, A. Kozłowski, Z. Tarnawski, E. Wilke, P. Babik, V. Chlan, R. Řezníček, H. Štěpánková, P. Novák, Y. Joly, J. Niewolski, and J. M. Honig, Phys. Rev. B **102**, 075126 (2020).

[11] R. Kukreja, N. Hua, J. Ruby, A. Barbour, W. Hu, C. Mazzoli, S. Wilkins, E. E. Fullerton, and O. G. Shpyrko, Phys. Rev. Lett. **121**, 177601 (2018).

[12] O. G. Shpyrko, E. D. Isaacs, J. M. Logan, Y. Feng, G. Aeppli, R. Jaramillo, H. C. Kim, T. F. Rosenbaum, P. Zschack, M. Sprung, S. Narayanan, and A. R. Sandy, Nature (London) **447**, 68 (2006).

[13] S. Konings, C. Schüßler-Langeheine, H. Ott, E. Weschke, E. Schierle, H. Zabel, and J. B. Goedkoop, Phys. Rev. Lett. **106**, 077402 (2011).

[14] S.-W. Chen, H. Guo, K. A. Seu, K. Dumesnil, S. Roy, and S. K. Sinha, Phys. Rev. Lett. **110**, 217201 (2013).

[15] X. M. Chen, V. Thampy, C. Mazzoli, A. M. Barbour, H. Miao, G. D. Gu, Y. Cao, J. M. Tranquada, M. P. M. Dean, and S. B. Wilkins, Phys. Rev. Lett. **117**, 167001 (2016).

[16] S. Yáñez-Vilar, E. D. Mun, V. S. Zapf, B. G. Ueland, J. S. Gardner, J. D. Thompson, J. Singleton, M. Sánchez-Andújar, J. Mira, N. Biskup, M. A. Señarís-Rodríguez, and C. D. Batista, Phys. Rev. B **84**, 134427 (2011).

[17] N. Lee, H. Y. Choi, Y. J. Jo, M. S. Seo, S. Y. Park, and Y. J. Choi, Appl. Phys. Lett. **104**, 112907 (2014).

[18] S. Chikara, J. Singleton, J. Bowlan, D. A. Yarotski, N. Lee, H. Y. Choi, Y. J. Choi, and V. S. Zapf, Phys. Rev. B **93**, 180405(R) (2016).

[19] H. Y. Choi, J. Y. Moon, J. H. Kim, Y. J. Choi, and N. Lee, Crystals **7** (2017).

[20] Y. Kamiya and C. D. Batista, Phys. Rev. Lett. **109**, 067204 (2012).

[21] V. S. Zapf, B. G. Ueland, M. Laver, M. Lonsky, M. Pohlit, J. Müller, T. Lancaster, J. S. Möller, S. J. Blundell, J. Singleton, J. Mira, S. Yañez-Vilar, and M. A. Señarís-Rodríguez, Phys. Rev. B **93**, 134431 (2016).

[22] See Supplemental Material at http://link.aps.org/supplemental/10.1103/PhysRevB.103.L060401 for a discussion of experimental details, heat capacity data, additional XPCS data, and analysis such as details of the ROIs, energy dependencies of scattering peaks, a second set of XPCS data taken during a separate beam time, and, finally, additional Monte Carlo simulations for the single-ion model and for a 3D case.

[23] C. Detlefs, M. Sanchez del Rio, and C. Mazzoli, Eur. Phys. J. Spec. Top. **208**, 359 (2012).

[24] N. Otsu, IEEE Trans. Syst., Man, Cybern. **9**, 62 (1979).

[25] L. T. Coutrim, D. Rigitano, C. Macchiutti, T. J. A. Mori, R. Lora-Serrano, E. Granado, E. Sadrollahi, F. J. Litterst, M. B. Fontes, E. Baggio-Saitovitch, E. M. Bittar, and L. Bufaiçal, Phys. Rev. B **100**, 054428 (2019).

[26] T. Moyoshi, R. Takahashi, and K. Motoya, J. Phys.: Conf. Ser. **273**, 012125 (2011).

[27] S. Agrestini, C. L. Fleck, L. C. Chapon, C. Mazzoli, A. Bombardi, M. R. Lees, and O. A. Petrenko, Phys. Rev. Lett. **106**, 197204 (2011).